High frame rate flow measurement using Ultrasound Imaging Velocimetry

Hogendoorn, Willian; Poelma, Christian

DOI
10.18726/2019_3

Publication date
2019

Document Version
Final published version

Published in
Proceedings of the 13th International Symposium on Particle Image Velocimetry (ISPIV 2019)

13th International Symposium on Particle Image Velocimetry – ISPIV 2019
Munich, Germany, July 22-24, 2019

High frame rate flow measurement using Ultrasound Imaging Velocimetry

Willian Hogendoorn[1*], **Christian Poelma**[1]

[1] Delft University of Technology, Multiphase Systems (3ME-P&E), 2628 CA Delft, The Netherlands

[*] W.J.Hogendoorn@tudelft.nl

Abstract

Using ultrasound in plane wave imaging mode, in combination with a proper processing strategy and the covariance function approach, we can not only better estimate the actual turbulence statistics, but we are also able to measure turbulent flows with much higher Reynolds numbers. Optimising the processing strategy by using a sliding correlation average of a few frames is significantly improving the signal-to-noise ratio, with an acceptable decrease in temporal resolution. With the covariance function approach we are able to distinguish noise and signal from each other. This improves the estimation of the actual turbulence statistics. In this study, turbulent pipe flow data for two different Reynolds numbers (5300 and 44000) is compared with literature. For both cases a good agreement is found for the mean velocity profile. Especially in the near-wall region, the estimation for u-rms is improved significantly. For the radial velocity fluctuations, a systematic underestimation is found, which is most likely due to the small displacements in this direction.

1 Introduction

Ultrasound Imaging Velocimetry (UIV) has proven to be a reliable non-intrusive measurement technique. Especially for measurements in opaque flows, this ultrasound-based technique was found to be a good alternative to optical PIV, which fails already for a dispersed phase volume fraction beyond 0.5% (see e.g. Poelma (2017)). Recently, we applied UIV to particle-laden flows with concentrations up to 14%, still being able to obtain qualitative velocity information (Hogendoorn and Poelma (2018)).

A major disadvantage of UIV is the relatively low acquisition frequency, as images are build up line-by-line. The relatively low speed of sound becomes an issue, which results in a limit of maximally a few hundred images per second for a useful field-of-view. This problem can be addressed by applying ultrasound in plane wave imaging mode (Montaldo et al. (2009)). This increases the sample frequency by more than one order of magnitude, potentially giving the ability to measure faster flows (i.e. higher Reynolds numbers). Furthermore, for relatively slow flows it creates oversampled data, which can be leveraged to improve velocity estimation. However, this higher sample frequency comes at the cost of a lower signal-to-noise ratio (SNR) of the images.

In this study we compare data, obtained with plane wave imaging ultrasound with reference data, in order to answer the question whether the loss in signal-to-noise of plane wave imaging is worth it, compared to conventional ultrasound imaging.

2 Experimental method

In this section the experimental details are given. Firstly the flow facility used for this study is described. After a paragraph about the specifications and settings of the ultrasound system, the way how the ultrasound images are processed is explained. This section ends with a paragraph about the improvement of the signal-to-noise ratio in the obtained UIV results.

2.1 Flow facility

The experiments in this study are performed in the same pipe flow facility as described by Trip et al. (2012). Studies performed earlier, which will be used as a reference, are also conducted in similar facilities (e.g. Eggels et al. (1994), Gurung and Poelma (2016)). For a more elaborate description of the facility, the reader is referred to those studies. Briefly, the flow is driven by a Nakakin sanitary rotary pump, which is controlled by means of LabVIEW. This pump is connected to an inlet chamber, where the flow is conditioned. The main part of the facility is the pipe, with an inner diameter (D) of 40 mm and a total length of about 200D. This is much longer than the required development length for the (turbulent) Reynolds numbers used in this study. The pipe ends in a reservoir with a free surface. This reservoir is connected to the pump in order to close the loop. In this return pipe the flow-rate is measured by means of an ultrasonic flowmeter (Krohne Altometer UFS500).

Contrary to the aforementioned studies, measurements are now performed in the very downstream section of the pipe, 5D before the exit. Especially for this study a box is created, which fits exactly around the pipe. This box is filled with water, such that the pipe is fully submerged in the water. The linear array of the ultrasonic transducer is mounted slightly below the water surface. By doing so, a significant reduction of acoustic reflections in the ultrasound images is gained.

2.2 Ultrasound system

For this study we used a Verasonics Vantage 128^{TM} in combination with a linear probe (L11-5v). This probe is operated at a frequency of 10.41 MHz instead of the center frequency of 7.81 MHz to obtain a better (radial) resolution (0.074 mm). Furthermore, a bandwidth of 9-12 MHz is prescribed, as this gave a relatively good image quality after visual inspection. The probe consists out of 128 single elements, each with a pitch of 0.3 mm; this also defines the resolution in stream-wise direction. This results in a total length of 38.4 mm, as is the width of the field of view. Note that the resolution in radial and stream-wise direction is not equal. The depth of the field of view is set, such that the whole pipe, including pipe walls is visible, giving a total depth of 50 mm. The probe has an elevational focal depth of 18 mm, which is placed slightly below the upper pipe wall. The received signal is sampled at a frequency of 250 MHz and stored, as well as the converted B-mode images. The later are used for the particle displacement estimation, which is done by particle imaging velocimetry software.

As tracer particles, Vestosint particles (Degussa-Hüls, Frankfurt, Germany) are used. With a mean diameter of 56 μm and a density of 1.016 g/cm^3 these particles are found to be good flow tracers, as the Stokes relaxation time is negligible. In addition, the acoustic properties of these particles are found to give a good acoustic signal as well. In previous research, these particles are used for optical PIV measurements (Scarano and Poelma (2009)) as well as UIV measurements (Gurung and Poelma (2016)).

2.3 Processing of Ultrasound images

A typical snapshot of a flow with Vestosint tracer particles, captured with plane wave imaging ultrasound, can be seen in Fig. 1(a). This image is acquired in a turbulent pipe flow with a Reynolds number of 5300 ($Re = DU_b/\nu$, where U_b is the bulk flow velocity and ν the kinematic viscosity). For this specific Reynolds number a plethora of reference data is available. In Fig. 1(b), an instantaneous vector field is shown. The color in the background is representing the time-averaged velocity. This vector field was obtained by applying standard correlation-based techniques on two subsequent ultrasound images, using 20x42 pixel interrogation areas. Furthermore, 50% overlap between the interrogation windows is used. Outliers are removed using the normalised median test (Westerweel and Scarano (2005)). The first and last vector columns are deviating from the centre ones. This is due to the (dis)appearance of particles in these regions. Throughout this study those regions are neglected for this reason. Contrary to conventional ultrasound, no sweep correction is required for the determination of the velocity components.

For ultrasound imaging velocimetry the correlation peak does not always resembles a proper Gaussian signal. The consequence of this is an inaccurate sub-pixel fit, sometimes giving unphysical particle displacements. These unphysical displacements are labelled and subsequently interpolated in time. However, the percentage of these displacements is very small though, as in the time-series of the vector field shown only 0.05 percent is found.

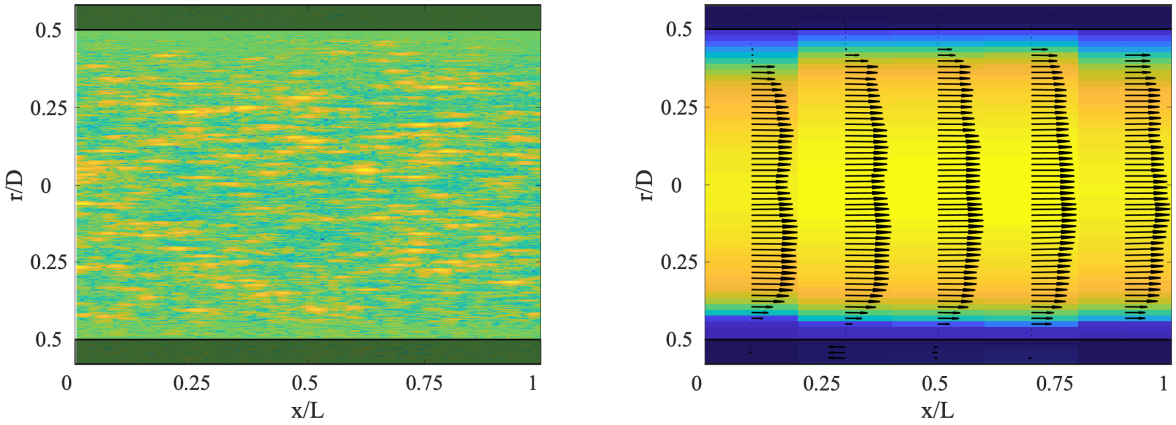

(a) Snapshot of a flow with tracer particles

(b) Instantaneous vector field

Figure 1: Example of plane wave imaging ultrasound.

2.4 Improvement of UIV results

For reliable turbulence statistics, the signal-to-noise ratio of the images is quantified first. For this a dataset with a sample frequency of 250 Hz is used, as this gives a good ratio of signal length (20 seconds) and temporal resolution. Signal and noise can be distinguished from each other via the covariance approach (Benedict and Gould (1996)). In this method, the time series of fluctuating velocity components is correlated at each radial location. An example is shown in Fig. 3(a), where data close to the pipe wall (r/R $\approx$ 0.9) is used, using a total of 4999 vector fields. Close to interfaces (such as pipe walls) the ultrasound signal is usually affected by acoustic reflections, resulting in a noisier signal. The peak at t = 0 is the sum of (uncorrelated) noise and turbulent fluctuations. This uncorrected value is what would be obtained by simply calculating the variance of the time series. By making use of the fact that the physical features (e.g. eddies) will be represented by a correlated signal, we can find a better estimate for the true fluctuations by extrapolating the covariance values to the ordinate axis (ignoring the covariance). For turbulent flows, classical theory predicts that the behaviour of the function for small delays will approach a parabola, which we use here to find the value marked 'corrected'. In this example the actual value is 15% lower than the raw signal would suggest. For the turbulence intensity, the square root of the variance must be taken, which comes down to an overestimation of 7% in this case.

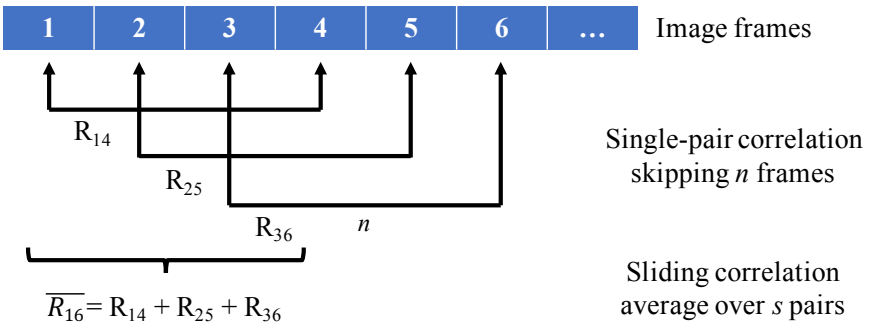

Figure 2: Schematic explanation of frame-skip (n) in combination with a sliding correlation average (s).

In addition to this covariance method, we used oversampled data as a leverage to reduce the noise peak in the covariance function. In order to find the most suitable processing strategy for this type of data we systematically varied two different parameters. This is schematically explained in Fig. 2, where six subsequent image frames are shown. The single-pair correlations are indicated with the arrows, where in this example three frames are skipped (n = 3). By using all six frames, three single-pair correlations are

determined, R_{14}, R_{25} and R_{36}. In order to improve the signal-to-noise ratio, these correlations are added, resulting in correlation $\overline{R_{16}}$. Throughout this paper we refer to this addition of correlations as 'sliding correlation average', where the number of single-pair correlations used for this sliding correlation average are denoted as 's'.

The signal-to-noise ratio as function of frame-skip and sliding correlation average is shown in Fig. 3(b). As can be seen is the signal-to-noise, for every single n, increasing when a sliding correlation average is used. This is in line with the expectations, as more data is used, a better result is obtained. Furthermore, for this specific case the best signal-to-noise ratio is found for a frame-skip of 4 and a sliding correlation average of 4. For small displacements (i.e. low n), the error introduced by the subpixel fit is relatively large, resulting in a bigger error. On the other hand the out-of-plane motion will be bigger for higher particle displacements, giving a noisier signal. The best result is found for n = 3-5, with a SNR of 5.7% for n = 4. In this case this gives an overestimation of the turbulence statistics of 2.8%.

In the next section we show that, by using both the covariance approach and the best sliding correlation average, reliable turbulence statistics could be obtained.

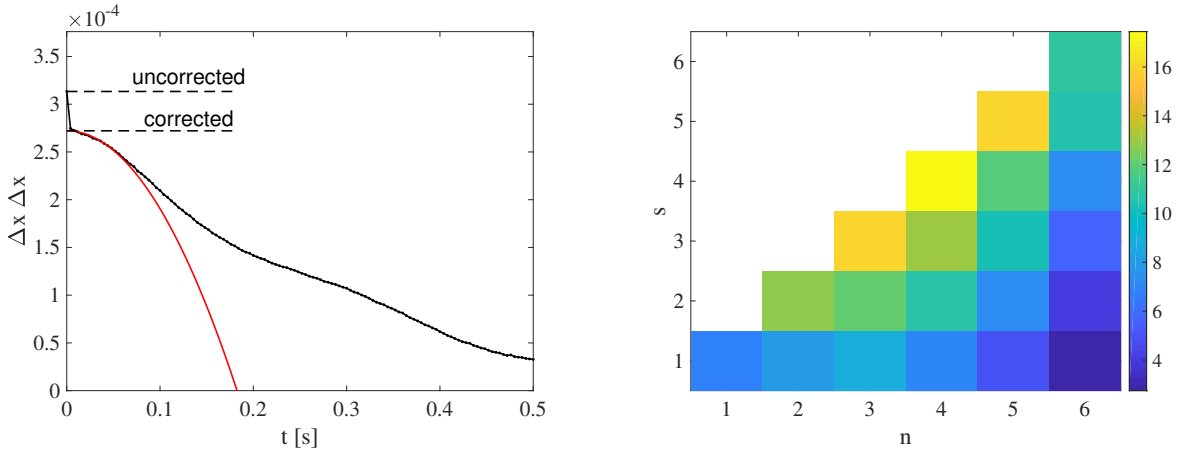

(a) Covariance function approach

(b) Signal-to-noise ratio as function of sliding average (s) and frame-skip (n)

Figure 3: Improvement of the signal-to-noise ratio for a time signal at radial position r/R ≈ 0.9.

3 Results: Comparison of turbulence statistics

In this section the results are discussed. For this study two different pipe flows, with different Reynolds numbers, are measured and compared with reference data. Both cases, Re = 5300 and Re = 44000 are discussed in Sect. 3.1 and Sect. 3.2, respectively.

3.1 Comparison with Re = 5300

The above described method is applied to five independent sets of data captured with a sample frequency of 250 Hz; in this case a frame-skip of 4 is used, resulting in an effective sample frequency of 62.5 Hz. Each set has a length of 20 seconds, giving a total length of 100 seconds. This is sufficiently long for a converged dataset, based on an integral timescale of 0.3 s. In the first place the average velocity profile (vector averaged) is compared with literature (Eggels et al. (1994)), and a good agreement is found, as can be seen in Fig. 4(a). As the flow is axisymmetric, the velocity profile shown is the average of the top and the bottom half velocity profile. This average is also applied in Fig. 4(b), where the stream-wise and radial velocity fluctuations are shown. These velocity fluctuations are normalised with the wall friction velocity. As pressure drop measurements are missing, the corresponding friction factor (which is required for the wall friction velocity) is determined by using Blasius's equation. For u-rms, the effect of the correction method, presented above is especially visible in the near-wall region. In this region acoustic reflections resulting from the pipe wall are reducing the signal of the passing tracer particles, resulting locally in noisier signal.

However, the corrected u-rms values are matching remarkably well with Eggels et al. (1994). For v-rms the correction applied is minor. Both the corrected and uncorrected signals are underestimating the reference curve. The reason for this is not clear yet. A possible explanation might be the small displacement of the particles in radial direction ($\approx$ 0.3 px), giving a relatively big uncertainty of the subpixel fit. Note the error bars in both curves, these represent the standard error, which is calculated based on the five different independent datasets.

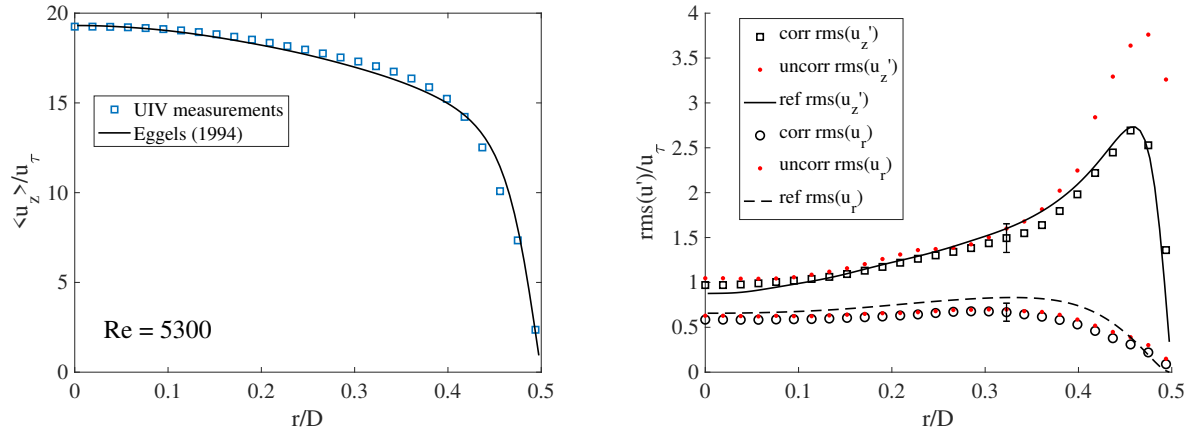

(a) Vector averaged velocity profile

(b) u-rms and v-rms profiles

Figure 4: Comparison of turbulence quantities with literature for a Reynolds number of 5300.

In addition to the turbulence statistics, a time-series of the turbulent flow is added, both for the stream-wise (Fig. 5(a)) and the radial (Fig. 5(b)) velocity components. Both signals are normalised with the time-averaged stream-wise centreline velocity (U_c). These time-series are obtained for a sample frequency of 500 Hz, with a sliding correlation average of 2, giving an effective time-resolution of 250 Hz. For this visualisation, the standard interrogation size of [20,42] is used, where only the vectors of the center-column (e.g. 3^{rd} column in Fig. 1(b)) are used. In addition, a median filter with a window size of [3x3] is used for a better visualization. Using Taylor's frozen turbulence hypothesis these time-series can also be interpreted as a spatial series, showing the turbulent structures in the pipe. The total time of 5 seconds corresponds to a length of around 16D, by scaling with the mean velocity.

3.2 Comparison with Re = 44000

In addition to the comparison with Re 5300, a comparison is made with reference data at a Reynolds number of 44000. In this case the data is compared with a direct numerical simulation study, performed by Wu and Moin (2008). For this comparison four independent datasets are used, which are captured with a sample frequency of 1000 Hz. The length of one dataset is 5 seconds; yielding a total length of 20 seconds. For an integral timescale of 0.042 seconds, there are enough eddies for converged statistics again. In this case a frame-skip and sliding correlation average of 2 was found to give the best result. For the averaged velocity profile (shown in Fig. 6(a)) a good comparison is found. For this comparison the velocity profile is normalised with the bulk flow velocity, U_b. The u-rms and v-rms profiles are shown in Fig. 6(b). Again, for the u-rms values close to the walls the uncorrected values are significantly over-predicting the reference curve. Using the covariance correction method, as described in Sect. 2.4, the corrected values are collapsing pretty well on the reference curve. For the values close to the pipe wall, there are only two points which are describing the strong gradients in that region. This will make it hard to show a trend in the signal over here. Comparing the fluctuations in radial direction (v-rms) with the reference, a systematic underestimation can be observed. Just as in the comparison in Sect. 3.1, this discrepancy is most likely due to the small displacements in this direction ($\approx$ 0.2 px). However, in this case the statistics are deviating more as compared to the previous case. This might be because of the sliding correlation average of 2, whereas in the previous case a sliding correlation average of 4 is used. A higher value will of course give a better signal-to-noise ratio, but in this case the sample frequency was not high enough to do so.

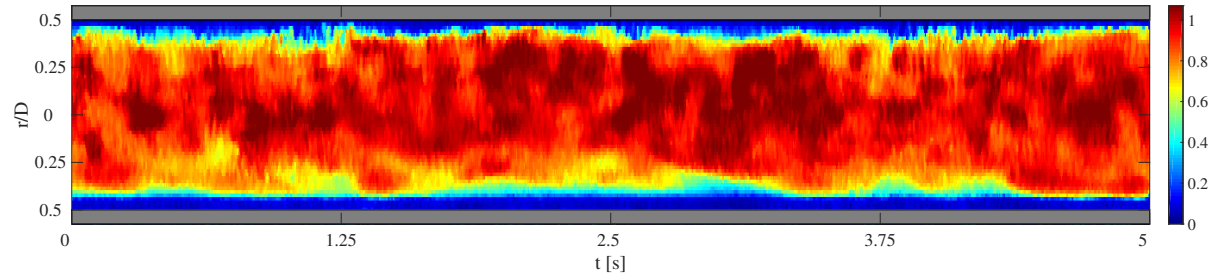

(a) Time serie of the stream-wise velocity component, u/U_c

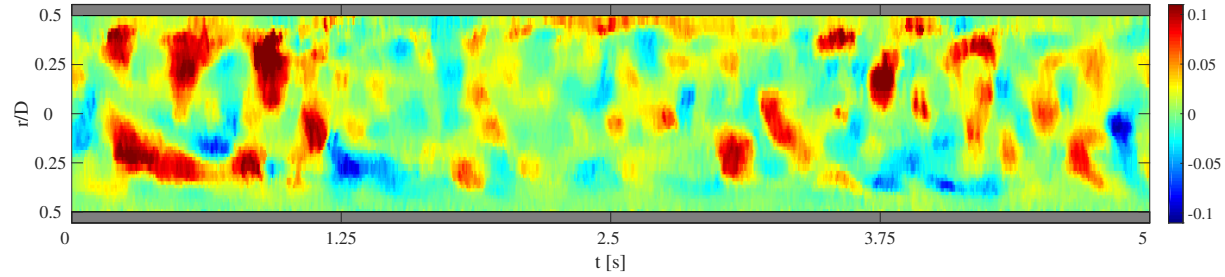

(b) Time serie of the radial velocity component, v/U_c

Figure 5: Stream-wise and radial velocity components in time for a Reynolds number of 5300.

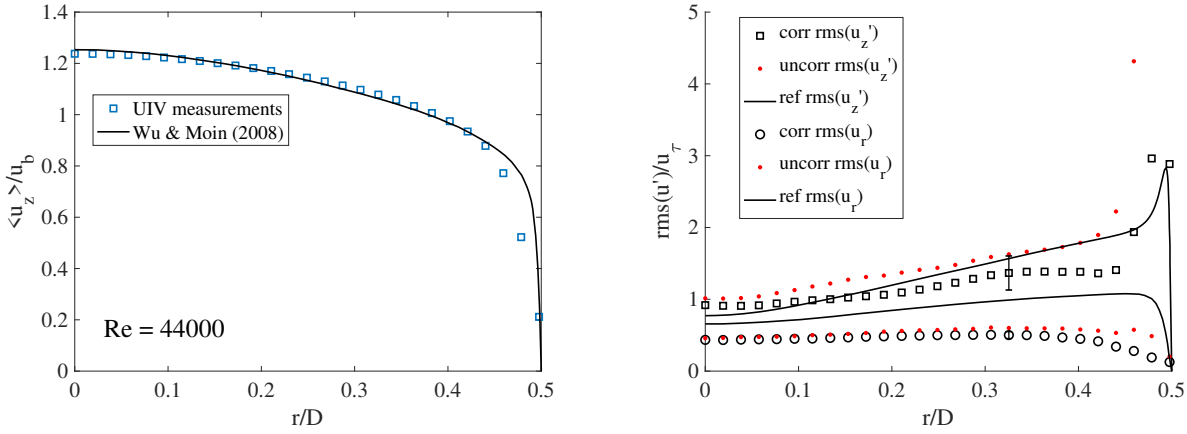

(a) Vector averaged velocity profile normalised with the bulk velocity

(b) u-rms and v-rms profiles

Figure 6: Comparison of turbulence quantities with literature for a Reynolds number of 44000.

For this case, a time-series of the turbulent flow is added as well. The result for the normalised stream-wise and radial velocity components are shown in Fig. 7(a) and 7(b), respectively. These time-series are obtained for a sample frequency of 2500 Hz, with a sliding correlation average of 2, giving an effective time-resolution of 1250 Hz. Also for this visualisation, the standard interrogation size of [20,42] is used, where only the vectors of the center-column (e.g. 3^{rd} column in Fig. 1(b)) are used. Mind that contrary to the case show in Fig. 5(a) and 5(b), the total duration of the time-series shown is 1 second only (corresponding to 24D). As expected are the turbulent fluctuations much more intense as compared to the previous (Re = 5300) case.

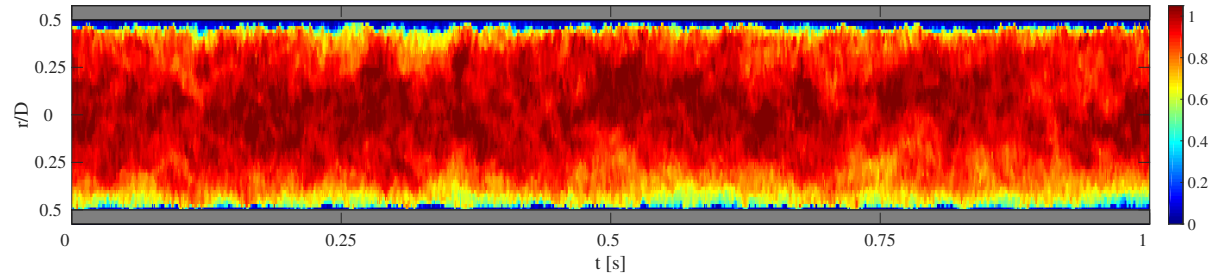

(a) Time serie of the stream-wise velocity component, u/U_c

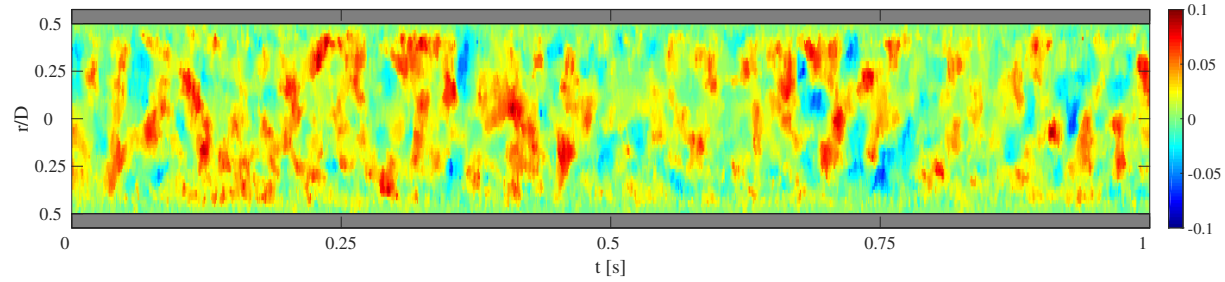

(b) Time serie of the radial velocity component, v/U_c

Figure 7: Stream-wise and radial velocity components in time for a Reynolds number of 44000.

4 Conclusion

In this study we compared two different turbulent flows, measured with ultrasound in plane wave imaging mode, with reference data. Using the covariance function approach in combination with an optimised processing strategy, we can better estimate the actual turbulence statistics. Especially in the near-wall regions, where acoustic reflections are spoiling the signal, the covariance approach is found to be a very helpful tool. A sliding correlation average of a few frames will improve the signal to noise ratio considerably, with an acceptable decrease in temporal resolution. Moreover, ultrasound applied in plane wave imaging mode is fast enough to achieve an acceptable temporal resolution. In conclusion, plane wave imaging ultrasound in combination with a proper processing strategy is able to measure higher Reynolds number flows as compared to a conventional ultrasound system. This also opens perspectives for quantitative measurements in opaque turbulent flows.

Acknowledgements

This work is funded by the ERC Consolidator Grant No. 725183 “OpaqueFlows.”

References

Benedict LH and Gould RD (1996) Towards better uncertainty estimates for turbulence statistics. *Experiments in Fluids* 22:129–136

Eggels J, Unger F, Weiss M, Westerweel J, Adrian R, Friedrich R, and Nieuwstadt F (1994) Fully developed turbulent pipe flow: a comparison between direct numerical simulation and experiment. *Journal of Fluid Mechanics* 268:175–210

Gurung A and Poelma C (2016) Measurement of turbulence statistics in single-phase and two-phase flows using ultrasound imaging velocimetry. *Experiments in Fluids* 57:171

Hogendoorn W and Poelma C (2018) Particle-laden pipe flows at high volume fractions show transition without puffs. *Physical review letters* 121:194501

Montaldo G, Tanter M, Bercoff J, Benech N, and Fink M (2009) Coherent plane-wave compounding for very high frame rate ultrasonography and transient elastography. *IEEE transactions on ultrasonics, ferroelectrics, and frequency control* 56:489–506

Poelma C (2017) Ultrasound imaging velocimetry: a review. *Experiments in Fluids* 58:3

Scarano F and Poelma C (2009) Three-dimensional vorticity patterns of cylinder wakes. *Experiments in Fluids* 47:69

Trip R, Kuik D, Westerweel J, and Poelma C (2012) An experimental study of transitional pulsatile pipe flow. *Physics of fluids* 24:014103

Westerweel J and Scarano F (2005) Universal outlier detection for piv data. *Experiments in fluids* 39:1096–1100

Wu X and Moin P (2008) A direct numerical simulation study on the mean velocity characteristics in turbulent pipe flow. *Journal of Fluid Mechanics* 608:81–112